Journal of Thermal Analysis and Calorimetry (2019) 138:4187–4195
https://doi.org/10.1007/s10973-019-08147-2

Structure, chemical stability and electrical properties of $BaCe_{0.9}Y_{0.1}O_{3-\delta}$ modified with V_2O_5

Agnieszka Lacz[1]

Received: 14 November 2018 / Accepted: 16 February 2019 / Published online: 2 March 2019

Abstract

Wet vacuum impregnation method was applied in order to evaluate the possibility of the formation of the material in $BaCe_{0.9}Y_{0.1}O_{3-\delta}$–$V_2O_5$ system. Single-phase $BaCe_{0.9}Y_{0.1}O_{3-\delta}$ samples, synthesised by solid-state reaction method, were impregnated with the solution of vanadium(V) oxide precursor. Multi-step, multi-cycle impregnation procedure was applied to enhance the impregnation efficiency. Partial decomposition of Y-doped $BaCeO_3$ in contact with the solution of the precursor, resulting in the formation of vanadium containing phases ($CeVO_4$ and BaV_2O_6) on the materials surface, was observed. However, the presence of vanadium was also confirmed for the inner parts of the materials. The synthesised materials were submitted for exposition test to evaluate their chemical stability towards CO_2/H_2O. All $BaCe_{0.9}Y_{0.1}O_3$-based materials modified by impregnation revealed higher chemical stability in comparison with single-phase un-modified $BaCe_{0.9}Y_{0.1}O_{3-\delta}$, since the amount of barium carbonate formed during the exposition was significantly lower. The total electrical conductivity of the received multi-phase materials was generally slightly lower than for the reference $BaCe_{0.9}Y_{0.1}O_{3-\delta}$ sample, since the presence of the additional phases had a blocking effect on materials conductivity. The values of $BaCeO_3$ lattice parameters and the Seebeck coefficient did not show the modification of the defects structure of Y-doped $BaCeO_3$ during applied synthesis procedure.

Keywords Chemical reactivity · Ceramic proton conductor · Vanadium(V) oxide · Barium cerate

Introduction

Synthesis of the composites based on doped $BaCeO_3$ is one of the main concepts concerning improvement of the chemical stability of $BaCeO_3$-based materials towards CO_2/H_2O containing atmosphere. It also results with modification of the materials microstructure and functional properties, mainly the transport properties—the mechanism and the value of conductivity. The synthesis of the composites is usually undertaken for doped barium cerate—doped ceria system, as the dopant yttrium, samarium, gadolinium or neodymium is frequently chosen [1–9]. However, the modification of doped $BaCeO_3$ with carbonates [10], tungstates [11] or phase rich in iron, nickel or titanium [12–14] was also reported.

In the area of the composites based on the perovskites, solid-state reaction or sol–gel methods are commonly used [3, 6, 8, 9, 15]. However, spark plasma sintering, chemical solution deposition, co-precipitation, citrate–nitrate combustion or impregnation can also be applied [1, 4, 11, 16, 17]. Two different approaches in the composites synthesis are usually undertaken. In the first one, the assumption is the single-step synthesis. In the second one, composite components are separately synthesised and the composite formation is performed by direct sintering or impregnation. For both cases, usually at least one of the synthesis steps requires the use of high temperature. Thus, undesirable processes connected with the mutual reactivity between the composites components and the co-doping of the perovskite structure materials can be observed, leading to the change of the materials defects structure [3, 5]. As the result, the decrease in the total conductivity and an increase in the activation energy of the conductivity are

✉ Agnieszka Lacz
alacz@agh.edu.pl

[1] Faculty of Materials Science and Ceramics, AGH University of Science and Technology, al. Mickiewicza 30, 30-059 Kraków, Poland

often seen [1–4]. In this work, an introduction of an additional phase into the sintered Y-doped $BaCeO_3$ was performed by low-temperature impregnation of the sintered perovskite with the solution of V_2O_5 precursor. Thus, only the solvent evaporation and the precursor decomposition at temperature below 500 °C had to be performed. Necessity of application of the relatively low temperatures should reduce cations interdiffusion and the materials co-doping, as well as the mutual reactivity between the components of the potential composite. Introduction of an additional phase often leads to the increase in the $BaCeO_3$-based materials chemical stability in corrosive CO_2/H_2O-rich atmospheres [1, 4, 11], but the decrease in electrical conductivity due to high contact resistance between both composites phases was also reported [2, 4]. Thus, vanadium(V) oxide was chosen as the modifier since its positive effects on both stability and conductivity of phosphate glasses were previously observed [18, 19].

Experimental

Single-phase Y-doped $BaCeO_3$ ($BaCe_{0.9}Y_{0.1}O_{3-\delta}$) was synthesised by solid-state reaction method. Barium carbonate, cerium(IV) oxide and 0.25 M water solution of yttrium nitrate (prepared based on $Y(NO_3)_3$ $6H_2O$) were used as the reagents. The $BaCO_3$ and CeO_2 powders' mixture was impregnated with the proper amount of yttrium nitrate solution and dried for 12 h at 80 °C. The received powder was calcined at 1200 °C for 24 h and then homogenized by milling in the absolute alcohol suspension using a rotation-vibration mill (operated in clockwise and anticlockwise rotation, total time of milling 1 h, speed 400 rpm) with ZrO_2 grinding media and dried at 90 °C for 24 h. The final powder was formed in the pellet dies (ϕ = 10 mm, thickness about 4 mm) at 2.5 MPa and sintered at 1300 °C for 3 h in air. Surface of the sintered $BaCe_{0.9}Y_{0.1}O_{3-\delta}$ pellets was ground using diamond paper and subsequently polished prior to all further investigations and synthesis steps in order to remove the CeO_2-rich phases formed on the surface as the result of barium oxide evaporation during sintering. The total porosities of $BaCe_{0.9}Y_{0.1}O_{3-\delta}$ samples determined on the basis of geometric measurements and samples' mass were equal to 32 ± 1 vol%. The vanadyl acetylacetonate dissolved in methanol (the solutions' concentration 0.35 M) was applied as the precursor of V_2O_5. Wet vacuum impregnation method was applied to introduce the V_2O_5 precursor solution into the sintered $BaCe_{0.9}Y_{0.1}O_{3-\delta}$.

Phase composition and unit cell parameters were determined based on XRD measurements taken on Philips X'Pert Pro diffractometer with monochromatized Cu-Kα. The Rietveld refinement was used for quantitative analysis. Scanning electron microscopy (SEM) (Nova NanoSEM 200 FEI) coupled with X-ray energy-dispersive spectroscopy (EDAX company apparatus) was used to observe the samples morphology and to determine their chemical composition. These measurements were taken on the samples polished cross sections.

The exposition test: long term (700 h), low-temperature (25 °C) exposure for CO_2/H_2O atmosphere (10% CO_2 and 100% HR) was performed on the received materials in order to evaluate the chemical stability towards carbon dioxide and water vapour. The un-modified $BaCe_{0.9}Y_{0.1}O_{3-\delta}$ and materials modified by impregnation in the form of pellets were exposed to this corrosive atmosphere in the custom-made degradation chamber. To analyse the exposition test results, samples before and after the test were submitted for thermogravimetric measurements taken on SDT2960 TA Instruments apparatus. The samples with mass about 50 mg were placed in the platinum crucibles and heated in synthetic air atmosphere with 10 deg min^{-1} heating rate.

The DC resistance and Seebeck coefficient measurements were performed in a Fine Instruments apparatus. The measurements were taken by Keysight Technology multimeter in fully automatic system in synthetic air as a function of temperature (250–700 °C). Before each measurement, the samples were stabilized at given temperature for 30 min. The conductivity was calculated based on measured resistance and sample geometry.

Results and discussion

Sample preparation

Wet impregnation under pressure method was applied to introduce additional components into the intergranular voids of the sintered single-phase $BaCe_{0.9}Y_{0.1}O_{3-\delta}$. The selection of the proper solution for impregnation was performed experimentally. The relatively high solubility in non-aqueous solvent was the main requirement, since the chemical resistance of barium cerate towards water is significantly small. The vanadyl acetylacetonate was chosen as the V_2O_5 precursor since it decomposes in air at relatively low temperature (about 400 °C) with formation of vanadium(V) oxide [20, 21]. Methanol was used as a solvent since it allowed a solution with relatively high concentration (0.35 M) to be obtained. Concerning the relatively high porosity of sintered $BaCe_{0.9}Y_{0.1}O_{3-\delta}$ (above 30%), the impregnation was performed under the pressure of 0.1 MPa. The higher pressure could lead to the mechanical destruction of the samples, especially that multi-step, multi-cycle impregnation was applied. Figure 1 presents the one cycle of impregnation. The

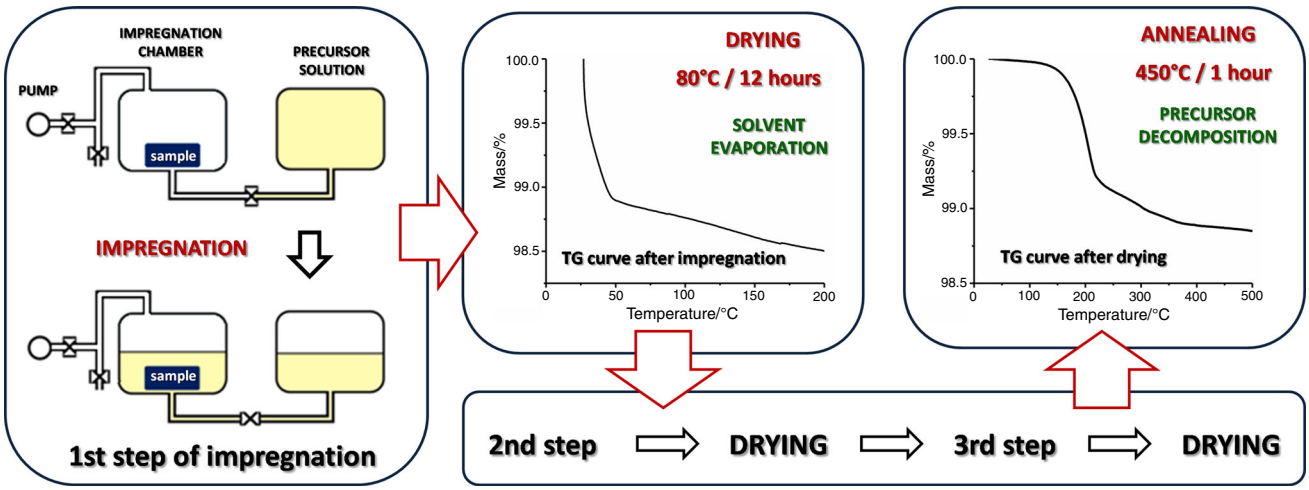

Fig. 1 Scheme of the one cycle of impregnation (I impregnation cycle) of $BaCe_{0.9}Y_{0.1}O_{3-\delta}$ with methanol solution of vanadyl acetylacetonate

$BaCe_{0.9}Y_{0.1}O_{3-\delta}$ samples before impregnation were dried (120 °C for 12 h) to remove the moisture and weighted. Single-phase $BaCe_{0.9}Y_{0.1}O_{3-\delta}$ samples impregnated with the solution of V_2O_5 precursor in methanol were drying at 80 °C for 12 h in order to evaporate the solvent. Then they were one more time impregnated (2nd step) and dried (80 °C, 12 h). This step was followed by 3rd impregnation and another drying. After three steps of impregnation, samples were annealed at 450 °C for 1 h to decompose vanadyl acetylacetonate to vanadium(V) oxide. This procedure was considered as the one cycle of impregnations (I impregnation cycle). For some samples, this procedure was repeated for the second time and for the third time. Thus, samples after I impregnation cycle (3 impregnations), II impregnation cycle (6 impregnations) and III impregnation cycle (9 impregnations) were obtained. In the following part of the paper, these samples will be labelled: BCYO_VO1, BCYO_VO2 and BCYO_VO3, respectively. For the reference single-phase $BaCe_{0.9}Y_{0.1}O_{3-\delta}$, the acronym BCYO will be used. The drying and annealing conditions were determined based on recorded TG curves.

To monitor the amount of compound introduced into the $BaCe_{0.9}Y_{0.1}O_{3-\delta}$, all samples were weighted after each drying and annealing process. The assumption was to synthesise the materials in $BaCe_{0.9}Y_{0.1}O_3$ - V_2O_5 system; thus, the recorded masses were used to evaluate the nominal composition of the received materials (Table 1).

Table 1 Nominal composition of received $BaCeO_3$-based materials

Samples name	Nominal composition/mole fraction	
	$BaCe_{0.9}Y_{0.1}O_3$	V_2O_5
BCYO_VO1	0.994	0.006
BCYO_VO2	0.987	0.013
BCYO_VO3	0.979	0.021

Structure, phase composition and microstructure

Single-phase $BaCe_{0.9}Y_{0.1}O_{3-\delta}$ with orthorhombic structure (space group *Pnma*, ICSD card no. 98-007-9625) was impregnated with the methanol solution of V_2O_5 precursor. In Fig. 2, the XRD results of the analysis of samples'

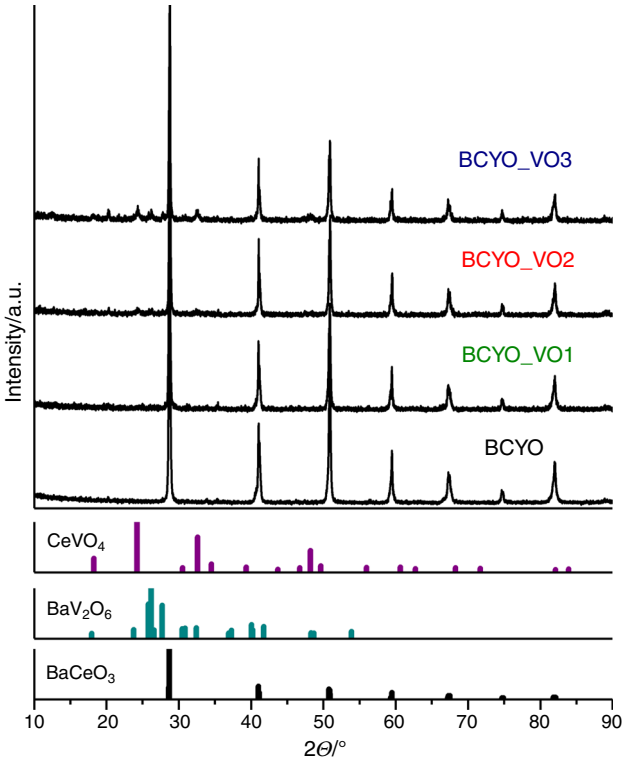

Fig. 2 XRD results of the initial $BaCe_{0.9}Y_{0.1}O_{3-\delta}$ sample and $BaCe_{0.9}Y_{0.1}O_{3-\delta}$ samples after impregnation

surface after I, II and III impregnation cycle are presented together with the results for $BaCe_{0.9}Y_{0.1}O_{3-\delta}$ sample before impregnation, as the reference. The analysis of diffractograms showed, in the case of all synthesized materials, the presence of orthorhombic (space group *Pnma*) $BaCeO_3$ as the main phase. Additional phases tetragonal $CeVO_4$ (space group *I41/amd*, ICSD card no. 01-072-0282) and orthorhombic BaV_2O_6 (space group *C222*, ICSD card no. 01-086-0240) were observed for BCYO_VO2 and BCYO_VO3 materials. The presence of these phases clearly indicates the decomposition of Y-doped $BaCeO_3$ in contact with methanol solution or during the precursor decomposition. The phase composition of the obtained materials in mole fraction, calculated based on the results of the Rietveld refinement, is presented in Table 2.

The increase in the content of the additional phases with the impregnation cycles suggests progressive decomposition of the perovskite. The relatively high content of $CeVO_4$ and BaV_2O_6 in comparison with assumed materials' composition indicates their segregation on the samples surface.

The $BaCeO_3$ lattice parameters for initial single-phase $BaCe_{0.9}Y_{0.1}O_{3-\delta}$ sample and impregnated $BaCe_{0.9}Y_{0.1}O_{3-\delta}$ samples (Table 3) are significantly comparable. Thus, eventual co-doping of Y-doped $BaCeO_3$ with vanadium or other changes in the chemical composition of the perovskite is excluded.

SEM microphotographs of pellets polished cross sections recorded for modified $BaCe_{0.9}Y_{0.1}O_{3-\delta}$ samples show porous materials with irregular pore structure (Fig. 3). EDS spectra indicate the presences of vanadium at the surface and in the interior parts of the materials. For the surface part of the samples, the increase in the number of the impregnation cycles leads to higher vanadium content. It stays in agreement with the results of XRD measurements indicating segregation of vanadium rich phases on the samples surface. For all modified $BaCe_{0.9}Y_{0.1}O_{3-\delta}$ materials, the small vanadium amount was also observed in the interior part of the materials. It suggests that applied impregnation method allows locating the additional vanadium-based phase not only on the materials surface. However, it must be noticed that due to the limitations of EDS method presented values should be treated for comparison only but not as absolute values.

Table 2 Phase composition of modified $BaCeO_3$-based materials

Sample	Phase composition/mole fraction		
	$BaCeO_3$	$CeVO_4$	BaV_2O_6
BCYO_VO1	1.0	–	–
BCYO_VO2	0.824	0.106	0.070
BCYO_VO3	0.647	0.209	0.144

Table 3 Lattice parameters of the initial and modified $BaCe_{0.9}Y_{0.1}O_{3-\delta}$

Sample	*a*/Å	*b*/Å	*c*/Å
BCYO	6.2163	8.7729	6.2367
BCYO_VO1	6.2165	8.7727	6.2366
BCYO_VO2	6.2163	8.7724	6.2370
BCYO_VO3	6.2168	8.7725	6.2364

Chemical stability

It is well known that the main disadvantage of Y-doped $BaCeO_3$ is the poor chemical stability in the CO_2 and water vapour-rich atmosphere [22–24]. Thus, the good electrical properties of these materials, including the proton conductivity, cannot be fully exploited since the materials relatively easily undergo chemical degradation resulting in the decrease in both mechanical and transport properties. To evaluate the chemical stability of synthesised materials, samples were exposed to carbon dioxide and water vapour-rich atmosphere (10% CO_2, 100% HR). During this long time (700 h), low-temperature (25 °C) exposition physical processes, e.g., adsorption of H_2O and/or CO_2 and chemical reaction between the material and a surrounding atmosphere can process. As it was discussed in the literature, Y-doped $BaCeO_3$ in CO_2/H_2O atmosphere can undergo degradation leading to the formation of $BaCO_3$ and $Ba(OH)_2$ [25, 26]. Thus, the phase composition of the material before and after the exposition can be different. TG curves for single-phase $BaCe_{0.9}Y_{0.1}O_{3-\delta}$ and $BaCe_{0.9}Y_{0.1}O_{3-\delta}$ modified by impregnation before and after the exposition test are presented in Fig. 4.

For all materials before the test, only one mass loss in the temperature range 500–800 °C is observed. This effect can be attributed to degradation of the protonic defects created in the perovskite as the result of yttrium doping [27, 28]. The shape of TG curves after the exposition is significantly different, since a few additional effects are clearly seen, where desorption of H_2O/CO_2 and decomposition of $BaCO_3$ formed during the explosion are the main one. The first one takes place below 400 °C, the second one at temperatures above 800 °C. This temperature is reported in the literature as the temperature of barium carbonate decomposition; however, it strongly depends on the surrounding atmosphere [29]. The total mass loss for single-phase $BaCe_{0.9}Y_{0.1}O_{3-\delta}$ is 3.8%, while for modified materials the total mass loss is 2.4%, 2.2% and 1.8% for BCYO_VO1, BCYO_VO2 and BCYO_VO3,

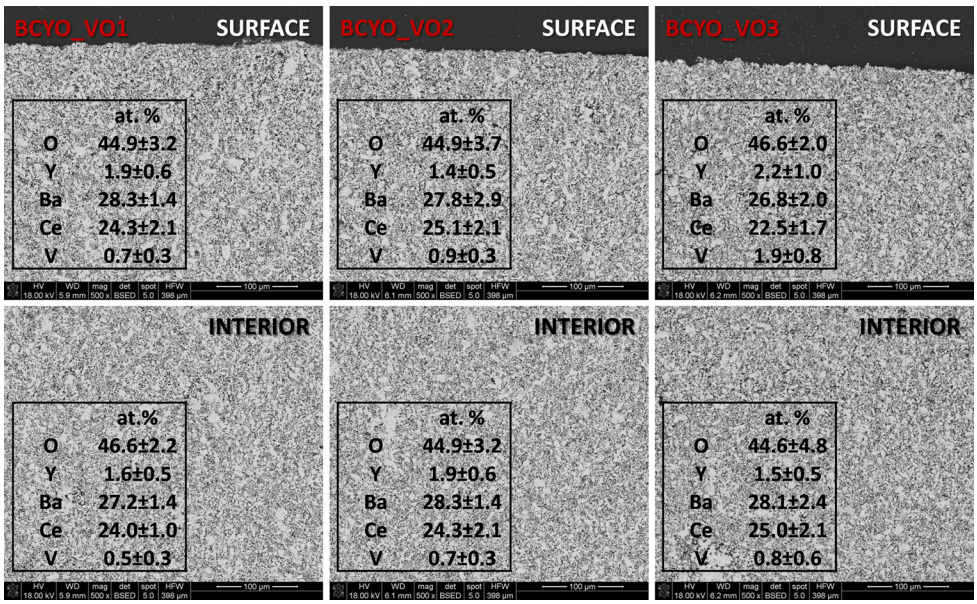

Fig. 3 SEM microphotographs of the cross section of the modified $BaCe_{0.9}Y_{0.1}O_{3-\delta}$ samples together with results of the EDS analysis

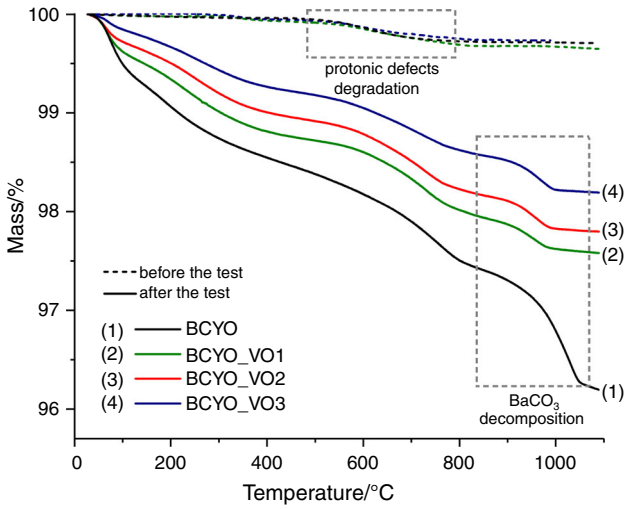

Fig. 4 TG curves for initial $BaCe_{0.9}Y_{0.1}O_{3-\delta}$ sample and modified $BaCe_{0.9}Y_{0.1}O_{3-\delta}$ samples before and after the exposition test

respectively. Based on the mass loss above 800 °C, the amount of $BaCO_3$ in the samples after the exposition was calculated. The barium carbonate content was 5.9% for single-phase $BaCe_{0.9}Y_{0.1}O_{3-\delta}$ and about 1.9–2.0% for modified materials. Thus, it can be postulated that $BaCe_{0.9}Y_{0.1}O_{3-\delta}$ materials after modification with the solution of V_2O_5 precursor are not completely stable in CO_2/H_2O-rich atmosphere; however, their stability is higher than stability of the single-phase $BaCe_{0.9}Y_{0.1}O_{3-\delta}$. As the reason of the perovskites' stability improvement, two factors are usually discussed, structure stabilization due to co-doping of $BaCe_{0.9}Y_{0.1}O_{3-\delta}$ and the presence of an additional phase. It was reported in the literature that incorporation of even a small amount of pentavalent ion (Nb^{5+}) into the barium cerate structure leads to significant improvement of the perovskite chemical stability due to the structure stabilization [30]. This co-doping should be followed by the change of the $BaCeO_3$ lattice parameters, as an ion with smaller ionic radii (Nb^{5+}, 0.78 Å CN = 6 [31]) is incorporated into Ce^{4+} position (1.01 Å for CN = 6 [31]). For $BaCe_{0.9}Y_{0.1}O_{3-\delta}$ modified by impregnation, the change of the lattice parameters compared to single-phase $BaCe_{0.9}Y_{0.1}O_{3-\delta}$ was not observed. Thus, co-doping of the perovskite structure cannot be considered as the reason of chemical stability improvement. The presence of the additional phases $CeVO_4$ and BaV_2O_6 is the most probable reason of the enhancement of stability towards CO_2/H_2O. As was discussed based on the XRD measurements results, materials received after impregnation were multi-phase except of BCYO_VO1 sample. Concerning the comparable chemical stability of BCYO_VO1 with the stability of BCYO_VO2 and BCYO_VO3 (similar content of barium carbonate), it can be postulated that even after only one impregnation cycle partial decomposition of the perovskite occurs and the additional phases are formed; however, their content is below the XRD detection point. The small differences between the mass losses for modified materials are mainly the reason of different amount of absorbed water, as the main difference is seen for temperatures below 100 °C. It cannot be excluded that the amount of secondary phases influence the possibility of water absorption, as the smaller

mass loss is observed for the material with the highest content of the additional phases (BCYO_VO3).

Electrical properties

Figure 5 presents the total electrical conductivities of modified $BaCe_{0.9}Y_{0.1}O_{3-\delta}$ materials in Arrhenius coordinates, together with the results for single-phase $BaCe_{0.9}Y_{0.1}O_{3-\delta}$ as the reference. Measurements were taken in synthetic air in the temperature range 250–700 °C. At these conditions ionic-hole transport occurs in Y-doped $BaCeO_3$ with the activation energy E_a of this total conductivity about 0.7–0.8 eV [32, 33]. Thus, the conductivity results for single-phase $BaCe_{0.9}Y_{0.1}O_{3-\delta}$ stay in general agreement with the literature data and the total conductivity observed is the result of oxide ion conductivity via oxygen vacancies and hole conductivity. According to the literature, $CeVO_4$ is the mixed ionic (oxygen ion) and p-type conductor, with the activation energy of conductivity about 0.4 eV [34, 35]. For barium vanadium oxide, the polaron hopping mechanism of conductivity was reported with the activation energy 0.89 eV [36]. The electrical conductivity of BCYO_VO3 sample is one–two orders of magnitude lower than that for the reference $BaCe_{0.9}Y_{0.1}O_{3-\delta}$. However, the activation energy for BCYO_VO3 sample (0.73 eV ± 0.02 eV) is comparable with the value observed for the reference (0.82 eV ± 0.03 eV); thus, the mechanism of the conductivity is rather not affected by the presence of the additional phases, especially that in both $BaCe_{0.9}Y_{0.1}O_{3-\delta}$ and $CeVO_4$ the similar mechanism of conductivity is observed. An observed slight decrease in the activation energy can be the result of lower activation energy for $CeVO_4$ conductivity. As was mentioned based on the XRD measurements results, the $CeVO_4$ and BaV_2O_6 phases are probably located at the samples surface. Thus, this decrease in the value of conductivity can be the result of the blocking effect of these vanadium rich phases on the total materials conductivity. This effect is also seen for the second multi-phase material (BCYO_VO2); however, the observed changes are non-monotonic. It suggests that after two cycles of impregnation with the methanol solution the surface of the sample is not fully covered by an uniform layer of the additional phases or the thickness of the layer is diverse; thus, the resultant effect is observed. According to the XRD measurements results, BCYO_VO1 sample is single-phase; however, exposition test results clearly imply the presence of an additional phase/phases. The electrical conductivity results also suggest the non-single-phase material, since the conductivity is lower than that for reference un-modified $BaCe_{0.9}Y_{0.1}O_{3-\delta}$.

Yttrium-doped $BaCeO_3$ and $CeVO_4$ are considered as mixed type conductors with the presence of p-type conductivity. The type of dominant carriers was confirmed by Seebeck coefficient measurements (Fig. 6). For all modified materials, similar as for reference $BaCe_{0.9}Y_{0.1}O_{3-\delta}$, the positive value of the Seebeck coefficient was observed. However, only for BCYO sample the Seebeck coefficient was measured with the high correlation (> 0.99) for the wide temperature range (450–700 °C). For BCYO_VO1, BCYO_VO2, BCYO_VO3 samples, the results with high correlation were obtained only for higher temperatures. Thus, the blocking effect related to the presence of the additional phases can also be considered.

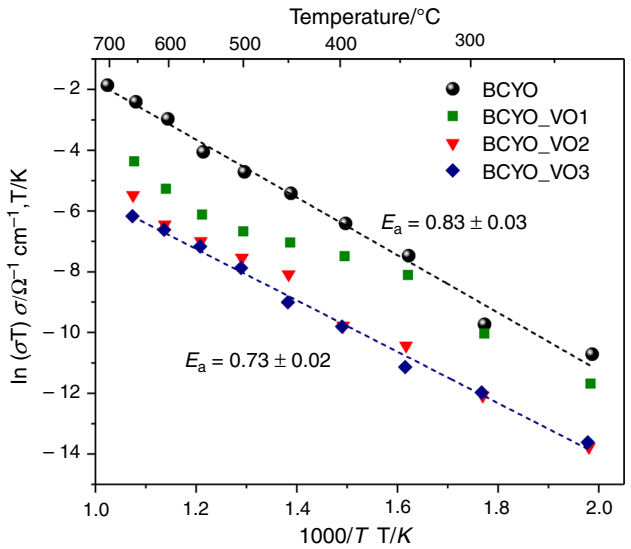

Fig. 5 Electrical conductivity of initial $BaCe_{0.9}Y_{0.1}O_{3-\delta}$ sample and modified $BaCe_{0.9}Y_{0.1}O_{3-\delta}$ samples in Arrhenius coordinates

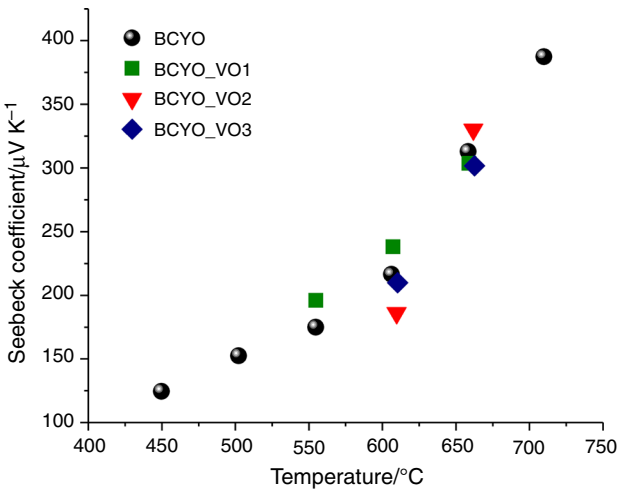

Fig. 6 Seebeck coefficient as a function of temperatures for initial $BaCe_{0.9}Y_{0.1}O_{3-\delta}$ sample and modified $BaCe_{0.9}Y_{0.1}O_{3-\delta}$ samples

Impregnation efficiency

The sample with the highest number of the impregnation procedures (BCVO_VO3) was chosen to evaluate the impregnation efficiency. Sample dimensions after III impregnation cycle were 9.90 mm in diameter and 3.80 mm in thickness. The surface of this pellet was polished on both sides using diamond paper to reduce the thickness for about 20%. As-prepared sample was submitted for XRD and electrical conductivity measurements. The main identified phase was orthorhombic $BaCeO_3$ (space group *Pnma*); however, small traces of additional phases tetragonal $CeVO_4$ (space group *I41/amd*) and rhombohedral $Ba_3V_2O_8$ (space group *R-3 m*, ICSD card no. 01-082-2057) were also observed (Fig. 7—only the position of peaks with the 100% intensity in the reference card for $CeVO_4$ and $Ba_3V_2O_8$ were indicated). The results clearly indicate that the applied impregnation method allows to introduce the precursor solution into the inner part of the sintered samples; nevertheless, it is still associated with the partial decomposition of the initial Y-doped $BaCeO_3$. The formation of barium-rich $Ba_3V_2O_8$ phase instead of BaV_2O_6 observed on the materials surface is probably the result of the smaller vanadium content.

The electrical conductivity of polished BCYO_VO3 sample was compared with the electrical conductivity of BCYO and BCYO_VO3 (Fig. 7). The general decrease in the conductivity was observed in comparison with single-phase $BaCe_{0.9}Y_{0.1}O_{3-\delta}$ material; however, the materials' conductivity was higher than for BCYO_VO3, where the relatively high content of additional phases was detected. Thus, the blocking effect of the vanadium containing phases on the total materials conductivity is clearly seen.

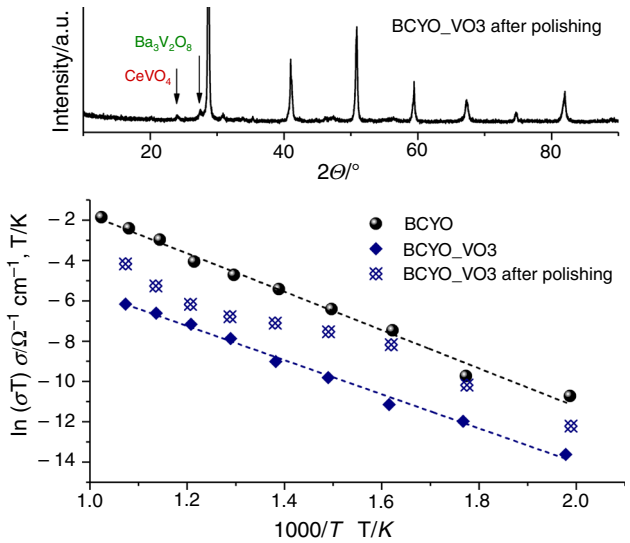

Fig. 7 Phase composition and electrical conductivity in Arrhenius coordinates of BCYO_VO3 samples after polishing

Moreover, the values of the conductivity and the shape of $\ln(\sigma T) = f(1000/T)$ dependency for BCYO_VO3 sample after polishing were similar to those observed for BCYO_VO1 sample. This is a further factor indicating the presence of the additional phases on the surface of the sample after only one impregnation cycle.

Conclusions

An attempt of introduction of an additional phase into the intergranular voids of sintered porous single-phase $BaCe_{0.9}Y_{0.1}O_{3-\delta}$ material by wet vacuum impregnation method was undertaken. The methanol solution of vanadyl acetylacetonate as the V_2O_5 precursor was applied. The procedure was performed in three cycles; each cycle consisted of three steps and the proper thermal treatment was applied to decompose the vanadyl acetylacetonate to V_2O_5. Unfortunately, during this synthesis procedure the $BaCe_{0.9}Y_{0.1}O_{3-\delta}$ undergoes partial decomposition; thus, $CeVO_4$ and barium vanadium oxides were observed as the additional phases, located mainly on the samples surface. However, vanadium containing phases were also seen in the inner parts of the materials. The $BaCeO_3$ lattice parameters calculated based on the XRD measurements results for initial single-phase $BaCe_{0.9}Y_{0.1}O_{3-\delta}$ and for modified materials proved that co-doping of Y-doped $BaCeO_3$ structure by vanadium does not occur. Also, the defects structure of the initial material was not changed since the presence of the proton defect was still observed for materials after impregnations.

Chemical stability of the obtained multi-phase materials towards CO_2 and water vapour was higher than for reference single-phase $BaCe_{0.9}Y_{0.1}O_{3-\delta}$ since the amount of $BaCO_3$ formed during the exposition test was lower for materials received by impregnation. Moreover, the smaller ability to absorption of gaseous was observed for modified material, probably as the result of segregation of the additional phases mainly on the materials surface. It was also the probable reason of the chemical stability improvement. The slight decrease in transport properties as the result of performed impregnations was observed, since the decrease in the total conductivity for modified materials was noticed in comparison with un-modified $BaCe_{0.9}Y_{0.1}O_{3-\delta}$. Still, the mixed oxide ion and hole conductivity were observed; however, the presence of the additional phases had a blocking effect on the total materials conductivity.

Acknowledgements This work was financially supported by National Science Centre Poland, Grant No. 2017/01/X/ST5/00789.

References

1. Gawel R, Przybylski K, Viviani M. Chemical stability and electrical properties of $BaCe_{0.85}Y_{0.15}O_{3-\delta}$–$Ce_{0.85}Y_{0.15}O_{2-\delta}$ composite bulk samples for use as central membrane materials in dual PCFC-SOFC fuel cells. Mater Chem Phys. 2014;147:804–14.
2. Medvedev D, Maragou V, Pikalova E, Demin A, Tsiakaras P. Novel composite solid state electrolytes on the base of $BaCeO_3$ and CeO_2 for intermediate temperature electrochemical devices. J Power Sources. 2013;221:217–27.
3. Khandelwal M, Venkatasubramanian A, Prasanna TRS, Gopalan P. Correlation between microstructure and electrical conductivity in composite electrolytes containing Gd-doped ceria and Gd-doped barium cerate. J Eur Ceram Soc. 2011;31:559–68.
4. Medvedev D, Pikalova E, Demin A, Podias A, Korzun I, Antonov B. Structural, thermomechanical and electrical properties of new $(1\text{-}x)Ce_{0.8}Nd_{0.2}O_{2-\delta}$–$xBaCe_{0.8}Nd_{0.2}O_{3-\delta}$. J Power Sources. 2014;267:269–79.
5. Wang H, Zhang L, Liu X, Bi H, Yu S, Han F, Pei L. Electrochemical study on $Ce_{0.85}Sm_{0.15}O_{1.925}$-$BaCe_{0.83}Y_{0.17}O_{3-\delta}$ composite electrolyte. J Alloy Compd. 2015;632:686–94.
6. Tian D, Liu W, Chen Y, Gu Q, Lin B. Low-temperature co-sintering of co-ionic conducting solid oxide fuel cells based on $Ce_{0.8}Sm_{0.2}O_{1.9}$-$BaCe_{0.8}Sm_{0.2}O_{2.9}$ composite electrolyte. Ionics. 2015;21:823–8.
7. Sun W, Jiang Y, Wang Y, Fang S, Zhu Z, Liu W. A novel electronic current-blocked stable mixed ionic conductor for solid oxide fuel cells. J Power Sources. 2011;196:62–8.
8. Ricote S, Manerbino A, Sullivan NP, Coors WG. Preparation of dense mixed electron- and proton-conducting ceramic composite materials using solid-state reactive sintering: $BaCe_{0.8}Y_{0.1}M_{0.1}O_{3-\delta}$–$Ce_{0.8}Y_{0.1}M_{0.1}O_{2-\delta}$ (M = Y, Yb, Er, Eu). J Mater Sci. 2014;49:4332–40.
9. Venkatasubramanian A, Gopalan P, Prasanna TRS. Synthesis and characterization of electrolytes based on $BaO\text{-}CeO_2\text{-}GdO_{1.5}$ system for intermediate temperature solid oxide fuel cells. Int J Hydrog Energy. 2010;35:4597–605.
10. Hei Y, Huang J, Wang C, Mao Z. Novel doped barium cerate-carbonate composite electrolyte material for low temperature solid oxide fuel cells. Int J Hydrog Energy. 2014;39:14328–33.
11. Lacz A, Pasierb P. Electrical properties and chemical stability of $BaCe_{0.9}Y_{0.1}O_3$-$BaWO_4$ composites synthesized by co-sintering and impregnation method. Solid State Ion. 2017;302:152–7.
12. Sun W, Fang S, Yan L, Liu W. Proton blocking composite cathode for proton-conducting solid oxide fuel cell. J Electrochem Soc. 2011;158:B1432–8.
13. Yang C, Zhang X, Zhao H, Shen Y, Du Z, Zhang C. Electrochemical properties of $BaZr_{0.1}Ce_{0.7}Y_{0.1}Yb_{0.1}O_{3-\delta}$–$Nd_{1.95}NiO_{4+\delta}$ composite cathode for protonic ceramic fuel cells. Int J Hydrog Energy. 2015;40:2800–7.
14. Fish JS, Ricote S, Lenrick F, Wallenberg LR, Holgate TC, O'Hayre R, Bonanos N. Synthesis by spark plasma sintering of a novel protonic/electronic conductor composite: $BaCe_{0.2}Zr_{0.7}Y_{0.1}O_{3-\delta}$/$Sr_{0.95}Ti_{0.9}Nb_{0.1}O_{3-\delta}$ (BCZY27/STN95). J Mater Sci. 2013;48:6177–85.
15. Cernea M, Vasile BS, Boni A, Iuga A. Synthesis, structural characterization and dielectric properties of Nb doped $BaTiO_3$/SiO_2 core–shell heterostructure. J Alloys Compd. 2014;587:553–9.
16. Kawabata Y, Sakamoto W, Yoshida K, Iijima T, Moriya M, Yogo T. Synthesis and characterization of multiferroic Pb(Zr, Ti)O_3/$CoFe_2O_4$/Pb(Zr, Ti)O_3 layered composite thin films by chemical solution deposition. J Ceram Soc Jpn. 2013;121:614–8.
17. Ghosh D, Han H, Nino JC, Subhash G, Jones JL. Synthesis of $BaTiO_3$-20 wt%$CoFe_2O_4$ nanocomposite via spark plasma sintering. J Am Ceram Soc. 2012;95:2504–9.
18. Pietrzak TK, Wasiucionek M, Gorzkowska I, Nowiński JL, Garbarczyk JE. Novel vanadium-doped olivine-like nanomaterials with high electronic conductivity. Solid State Ion. 2013;251:40–6.
19. Hong J, Wang CS, Chen X, Upreti S, Whittingham MS. Vanadium modified $LiFePO_4$ cathode for Li-ion batteries. Electrochem Solid State Lett. 2009;12:A33.
20. Van Der Voort P, White MG, Vansant EF. Thermal decomposition of $VO(acac)_2$ deposited on the surfaces of silica and alumina. Langmuir. 1998;14:106–12.
21. Nenashev RN, Mordvinova NE, Zlomanov VP, Kuznetsov VL. Thermal decomposition of vanadyl acetylacetonate. Inorg Mater. 2015;51:891–6.
22. Medvedev DA, Lyagaeva JG, Gorbova EV, Demin AK, Tsiakaras P. Advanced materials for SOFC application: Strategies for the development of highly conductive and stable solid oxide proton electrolytes. Prog Mater Sci. 2016;75:38–79.
23. Okiba T, Fujishiro F, Hashimoto T. Evaluation of kinetic stability against CO_2 and conducting property of $BaCe_{0.9-x}Zr_xY_{0.1}O_{3-\delta}$. J Therm Anal Calorim. 2013;113:1269–74.
24. Kim JH, Kang YM, Byun MS. Hwang KT Study on the chemical stability of Y-doped $BaCeO_{3-\delta}$ and $BaZrO_{3-\delta}$ films deposited by aerosol deposition. Thin Solid Films. 2011;520:1015–21.
25. Ryu KH, Haile SM. Chemical stability and proton conductivity of doped $BaCeO_3$–$BaZrO_3$ solid solutions. Solid State Ion. 1999;125:355–67.
26. Ma G, Shimura T, Iwahara H. Ionic conduction and nonstoichiometry in $Ba_xCe_{0.90}Y_{0.10}O_{3-\alpha}$. Solid State Ion. 1998;110:103–10.
27. Slodczyk A, Sharp MD, Upasen S, Colomban P, Kilner JA. Combined bulk and surface analysis of the $BaCe_{0.5}Zr_{0.3}Y_{0.16}Zn_{0.04}O_{3-\delta}$ (BCZYZ) ceramic proton-conducting electrolyte. Solid State Ion. 2014;262:870–4.
28. Pasierb P, Drożdż-Cieśla E, Gajerski R, Łabuś S, Komornicki S, Rękas M. Chemical stability of $Ba(Ce_{1-x}Ti_x)_{1-y}Y_yO_3$ proton-conducting solid electrolytes. J Therm Anal Calorim. 2009;96:475–80.
29. Earnest CM, Miller ET. An assessment of barium and strontium carbonates as temperature and enthalpy standards. J Therm Anal Calorim. 2017;130:2277–82.
30. Bartolomeo ED, D'Epifanio A, Pugnalini C, Giannici F, Longo A, Martorana A. Structural analysis, phase stability and electrochemical characterization of Nb doped $BaCe_{0.9}Y_{0.1}O_{3-x}$ electrolyte for IT-SOFCs. J Power Sources. 2012;199:201–6.
31. Shannon RD. Revised effective ionic radii and systematic studies of interatomic distances in halides and chaleogenides. Acta Cryst. 1976;A32:751–67.
32. Jadhav ST, Dubal SU, Jamale AP, Patil SP, Bhosale CH, Puri VR, Jadhav LD. Structural, morphological and electrical studies of $BaCe_{0.8}Y_{0.2}O_{3-\delta}$ synthesized by solution combustion method. Ionics. 2015;21:1295–300.
33. Chen Q, Braun A, Yoon S, Bagdassarov N, Graule T. Effect of lattice volume and compressive strain on the conductivity of BaCeY-oxide ceramic proton conductors. J Eur Ceram Soc. 2011;31:2657–61.
34. Watanabe A. Highly conductive oxides, $CeVO_4$, $Ce_{1-x}M_xVO_{4-x}$ (M = Ca, Sr, Pb) and $Ce_{1-y}Bi_yVO_4$, with zircon-type structure

prepared by solid-state reaction in air. J Solid State Chem. 2000;153:174–9.
35. Tsipis EV, Patrakeev MV, Kharton VV, Vyshatko NP, Frade JR. Ionic and p-type electronic transport in zircon-type $Ce_{1-x}A_xVO_{4\pm\delta}$ (A = Ca, Sr). J Mater Chem. 2002;12:3738–45.
36. El-Desoky MM. DC conductivity and hopping mechanism in V_2O_5–B_2O_3–BaO glasses. Phys Stat Sol. 2003;195:422–8.